

Novel calcined Mg-Cr hydrotalcite supported Pd catalysts for the hydrogenolysis of CCl_2F_2

A.H. Padmasri, A. Venugopal, J. Krishnamurthy, K.S. Rama Rao*, P. Kanta Rao

Catalysis and Physical Chemistry Division, Indian Institute of Chemical Technology, Hyderabad 500 007, India

Received 23 January 2001; received in revised form 28 March 2001; accepted 26 June 2001

Abstract

Pd supported on calcined Mg-Cr hydrotalcite, MgO and Cr_2O_3 are prepared and tested for the hydrogenolysis of CCl_2F_2 . It is found that 6 wt.% Pd loading is optimum on MgO- Cr_2O_3 hydrotalcite. The hydrogenolysis activities for CCl_2F_2 are found in the order: Pd/HT > Pd/MgO > Pd/ Cr_2O_3 . While Pd/HT is yielding deep hydrogenation product (CH_4) with more selectivity, Pd/MgO is yielding dechlorination product (CH_2F_2). Pd/ Cr_2O_3 is showing poor activity. It is observed that calcined Mg-Cr hydrotalcite has shown synergy when used as a support for Pd and used for the hydrogenolysis of CCl_2F_2 . © 2002 Elsevier Science B.V. All rights reserved.

Keywords: Hydrogenolysis; Mg-Cr hydrotalcite; CCl_2F_2 ; Pd catalysts; Synergy

1. Introduction

Hydrotalcite-like compounds (HTs) are well recognized as good catalysts and catalyst supports in catalyzing a variety of reactions and have been more extensively used as basic catalysts in reactions like aldol condensations, alkylations, polymerization [1], etc. and to a lesser extent as supports for noble-metal catalysts in different reactions like hydrogenation, partial oxidation and methanol decomposition to synthesis gas [2].

Hydrodechlorination of chlorofluorocarbons (CFCs) is one of the simplest and best routes for the synthesis of hydrofluorocarbons (HFCs), which involves the selective cleavage of C-Cl bond, using Pd based catalysts. Many authors have reported this reaction over Pd supported on different carriers like oxides (Al_2O_3 ,

TiO_2), fluorides (AlF_3 , ZrF_4), activated carbon and graphite [3,4]. Pd/ AlF_3 , Pd/ Al_2O_3 and Pd/C are reported as very selective and stable catalysts for this reaction. According to Kim et al. [5], Pt/MgO is a very stable and selective catalyst in the hydrodechlorination of CCl_4 to CHCl_3 . Also Pd/MgF₂ has been reported to be a good catalyst for the synthesis of CH_2F_2 by the hydrodechlorination of CCl_2F_2 [6] offering good stability and selectivity towards the desired product.

Pd/ Al_2O_3 and Pd/C are the commonly employed catalysts for the hydrodechlorination of CCl_2F_2 . But both the catalysts have their own merits and demerits. Al_2O_3 being acidic in nature can catalyze coking during the course of the reaction and also undergo transformation to aluminum oxy/hydroxy fluorides due to the release of HF. Carbon on the other hand has poor mechanical strength and its microporous nature can pose some problems particularly the active component present in its narrow pores may not be accessible for the reactant molecules for the reaction to occur.

* Corresponding author.

E-mail addresses: ksramarao@iict.ap.nic.in (K.S. Rama Rao), pkr@iict.ap.nic.in (P. Kanta Rao).

Hence, alternate catalytic systems are necessary for the hydrodechlorination of CCl_2F_2 (CFC-12).

In our recent study [7], we found calcined Mg-Al hydrotalcite supported Pd catalysts to be highly active and selective in the synthesis of HFC-32 by the hydrodechlorination of CFC-12. Mg-Al hydrotalcite is extensively studied as a catalyst for its versatile characteristics like high basicity, surface area and good thermal stability (although less extensively as a support). Mg-Cr hydrotalcite has also been reported to show similar reactivity and has been studied for the alkylation reaction as a catalyst [8] and as a support for Pd catalyst in the decomposition of methanol [2]. The present work is a study of hydrogenolysis of CCl_2F_2 over Pd supported on calcined Mg-Cr-HT catalysts with varying Pd loading from 1 to 10 wt.% and the aim of this work is to compare the hydrogenolysis activity of Pd/Mg-Cr HT with that of Pd/MgO and Pd/Cr₂O₃ catalysts.

2. Experimental

2.1. Preparation of catalysts

Mg-Cr hydrotalcite is prepared by the co-precipitation under super saturation conditions according to Reichle's method [9] and the product is calcined in N_2 at 723 K for 18 h. An amount of 1–10 wt.% Pd supported on calcined Mg-Cr hydrotalcite catalysts are prepared by the impregnation of requisite amount of acidified (with dil. HCl) aqueous PdCl_2 solution. MgO support is prepared by precipitation from aqueous $\text{Mg}(\text{NO}_3)_2$ with Na_2CO_3 followed by drying at 393 K for 12 h and then calcination in air for 18 h at 723 K. Cr₂O₃ support is prepared by slow addition of dilute ammonia to dilute aqueous solution containing $\text{Cr}(\text{NO}_3)_3 \cdot 9\text{H}_2\text{O}$ followed by filtration, washing and drying at 393 K for 12 h and subsequent calcination at 723 K in air for 18 h. Both MgO and Cr₂O₃ supports are used for the deposition of PdCl_2 with a Pd loading of 6 wt.%. All the dried catalyst samples after impregnation with PdCl_2 are calcined in N_2 at 723 K for 18 h and reduced in H_2 at 673 K for 3 h before the reaction.

2.2. Characterization

All the fresh and used catalysts have been characterized by XRD, BET surface area and TPR techniques.

The surface area measurements are done on an all glass high vacuum system by BET method (at 10^{-6} Torr) using N_2 adsorption at liquid N_2 temperature. XRD patterns of all the catalysts in this study are recorded at room temperature on a Siemens D5000 X-ray diffractometer using Ni filtered $\text{Cu K}\alpha$ radiation.

TPR studies are made on a home-made on-line system which consists of a quartz reactor placed in a metal block furnace equipped with a temperature programmer cum controller connected through a thermocouple and a GC with a thermal conductivity detector connected to data station for recording the profiles. About 150–200 mg of the catalyst sample (18/25 mesh sieved particles) is placed in the quartz reactor and packed in between quartz wool and heated at a ramp of 5 K min^{-1} from ambient temperature to 973 K by passing the reducing gas mixture (6% H_2 in argon) over the catalyst. The gas mixture from down the reactor is then passed through an alkali trap in order to remove any HCl/HF formed during the reduction process and then through a molecular sieve trap to remove the moisture and then let into the GC blank column connected to TCD for analyzing and recording the profiles.

2.3. Activity study

Hydrogenolysis of CCl_2F_2 over 1–10 wt.% Pd/cal Mg-Cr-HT, Pd/MgO and Pd/Cr₂O₃ has been carried out in a fixed bed micro reactor that is connected on-line to GC equipped with a FID detector at atmospheric pressure and at a reaction temperature of 523 K, and maintaining a molar ratio of $\text{H}_2/\text{CFC-12} = 8$ and at a gas hourly space velocity (GHSV) of 4000 h^{-1} . During a preliminary study, these reaction conditions have been found to be optimum to obtain good activity and selectivity. The products are analyzed under steady state conditions by GC using a Porapak-Q (3 m long and 1/8" diameter made of ss) column and confirmed by GC-MS analysis.

3. Results and discussion

Table 1 shows the BET surface areas of supports and catalysts (in fresh as well as used form). Decrease of surface area upon the deposition of Pd is well expected and this trend is observed on all the supported

Table 1
BET surface area of supports and supported Pd catalysts

S. no.	Catalyst	Pd loading (wt.%)	BET surface area ($\text{m}^2 \text{g}^{-1}$)	
			Fresh catalyst	Used catalyst
1	MgO	–	110	–
2	Cr_2O_3	–	240	–
3	HT	–	165	–
4	6Pd/MgO	6	92	27
5	6Pd/ Cr_2O_3	6	95	52
6	1Pd/HT	1	98	55
7	2Pd/HT	2	56	42
8	4Pd/HT	4	55	40
9	6Pd/HT	6	46	24
10	8Pd/HT	8	34	20
11	10Pd/HT	10	28	18

Pd catalysts. However, deposition of Pd on MgO does not decrease the surface area significantly. During the preparation of Pd/MgO catalyst migration of Cl^- ion on to MgO surface and decoration of MgO on Pd might have occurred, and therefore, no drastic decrease in the BET area is observed. Decoration of MgO

in the presence of Cl^- ion on Ru and Cu catalysts is reported [10]. The used catalysts recorded a decrease in their BET areas, mostly because of the transformation of oxidic supports into corresponding fluorides or hydroxyfluorides under the corrosive reaction conditions where liberation of HCl and HF occur.

Fig. 1 shows the XRD patterns of Mg-Cr hydrotalcite in dried and calcined forms and those of Pd/MgO, Pd/ Cr_2O_3 and Pd/HT (calcined) catalysts (fresh) with 6 wt.% Pd loading in each catalyst. Signals due to hydrotalcite structure, $\text{Mg}_6\text{Cr}_2(\text{OH})_{16}(\text{CO}_3^{2-}) \cdot 4\text{H}_2\text{O}$ (stichtite, d -values: 7.8₁₀₀, 3.91₉₀, 2.60₄₀, 1.54₂₀) are visible from the XRD pattern in dried form. Calcination at 723 K for 18 h destroys this structure and poorly crystalline structure due to MgO (ASTM card no. 4-829) is formed.

In the case of Mg-Al hydrotalcites, brucite like, positively charged layers of magnesium and aluminum hydroxide octahedral sharing edges with interstitial carbonate anions to charge compensate and water molecules between the metal hydroxide layers are present [11]. It was reported that interstitial water was lost reversibly below 473 K. Between 523

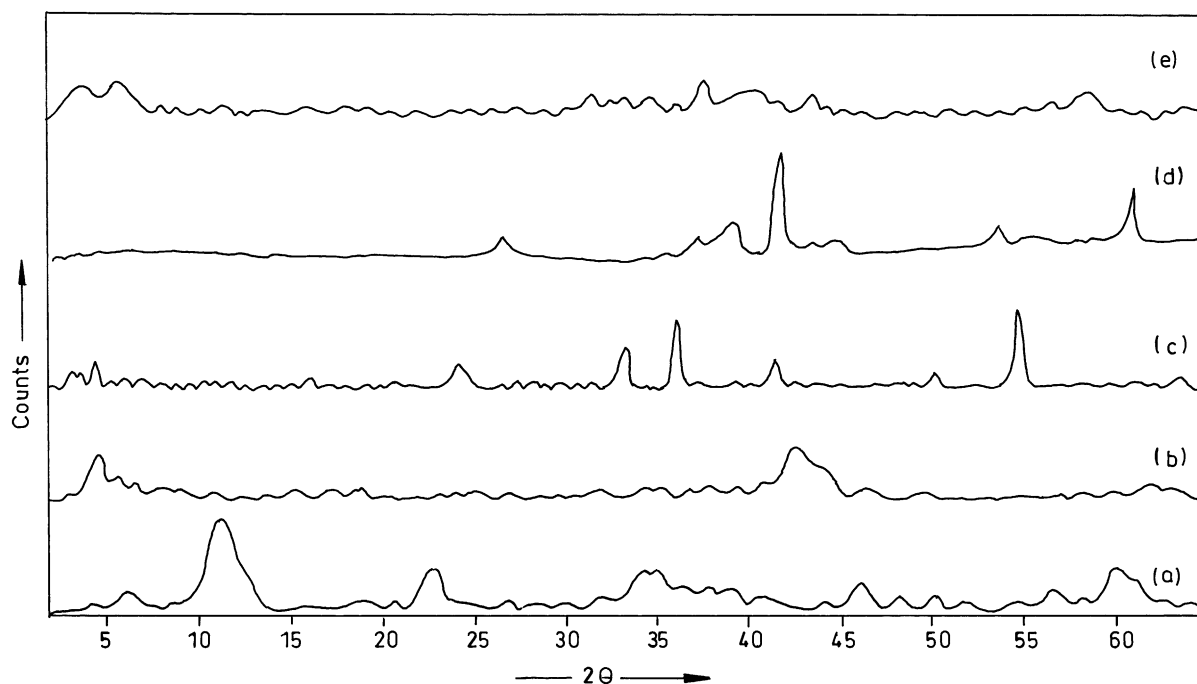


Fig. 1. XRD patterns of (a) Mg-Cr hydrotalcite, dried; (b) Mg-Cr hydrotalcite, calcined; (c) Pd/ Cr_2O_3 , fresh; (d) Pd/MgO, fresh; (e) Pd/HT, fresh.

and 723 K both carbon dioxide and water from the dehydroxylation were lost [12–14]. This reaction was also reversible. However, prolonged heating at higher temperatures results in yielding basic mixed oxides. Thus, in this investigation, calcining at 723 K for 18 h yielded poorly crystalline MgO with Cr₂O₃ in amorphous state. Shiozaki et al. [2] also observed the diffraction lines due to MgO only when a Mg-Cr HT was calcined in H₂ flow at 673 K. Thus, in this study, Mg-Cr hydrotalcite acts as a precursor to a mixture of MgO and Cr₂O₃ which are formed upon calcination prior to the deposition of Pd.

In Pd/MgO and Pd/Cr₂O₃ patterns (Fig. 1), XRD reflections due to respective supports can be clearly seen. XRD results of Pd containing HTs with different Pd contents indicate the presence of PdO and α -Pd phases whose intensities start increasing with increase in Pd loading. In the case of Pd/HT used catalysts, XRD phases due to α -Pd and MgF₂ are present in high intensities. Phases due to PdF₂, CrF₃·3H₂O are also present along with weak signals of MgO. Fluorinated phases due to the transformation of oxides during the course of reaction are expected.

TPR patterns of Pd/MgO, Pd/Cr₂O₃ and Pd/HTs (fresh) are shown in Fig. 2. H₂ consumption in the form a positive signal centered at a $T_{\max} \sim 453$ K can be seen in the TPR pattern of Pd/MgO catalyst. It is a known fact that bulk PdCl₂ is reduced in H₂ flow at room temperature forming β -PdH_x species which upon decomposition gives a negative signal during TPR run. PdCl₂ or most of other Pd precursors, which get reduced easily at room temperature in hydrogen atmosphere, result in developing an interaction between Pd metal and hydrogen. In fact the interaction between these two to form a PdH_x like species, is a subject of topic in the metallic membranes for an important technological application to separate hydrogen from gas mixtures. Lagos and co-workers [15–17] have explained the interaction between hydrogen and Pd metal as to subsurface bonding of hydrogen. According to his calculations on energy requirements, hydrogen would prefer to bind to subsurface sites of Pd rather than surface sites. The preferential absorption of hydrogen by these subsurface sites would facilitate hydrogen diffusion into the bulk of the metal. According to Van Hove and Hermann [18], sites on the top first Pd layer and between first and second Pd layer are surface sites and the interaction between

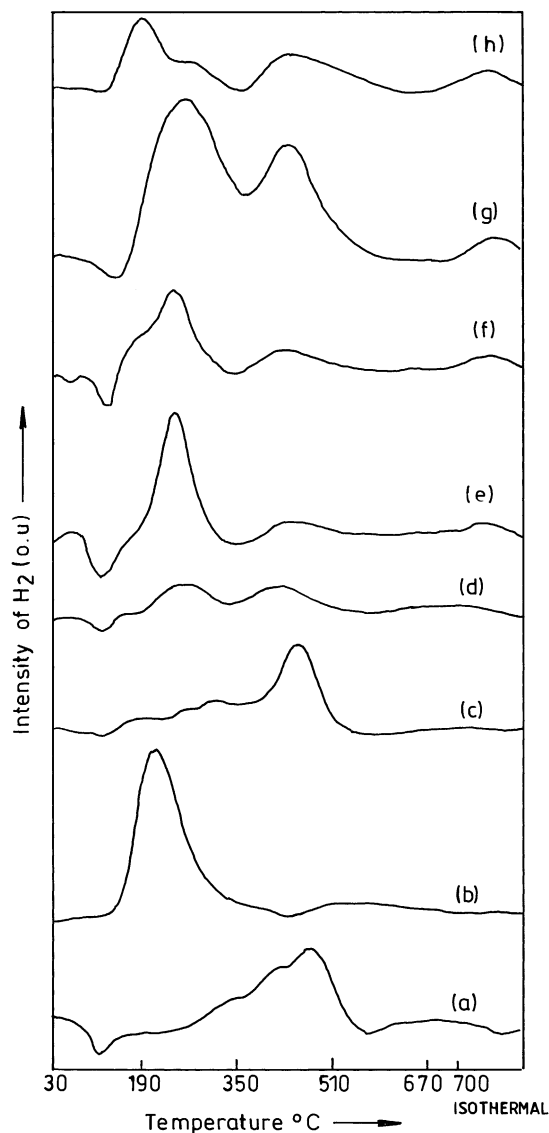


Fig. 2. TPR patterns of calcined fresh supported Pd catalysts: (a) 6% Pd/Cr₂O₃; (b) 6% Pd/MgO; (c) 1% Pd/HT; (d) 2% Pd/HT; (e) 4% Pd/HT; (f) 6% Pd/HT; (g) 8% Pd/HT; (h) 10% Pd/HT.

these sites with hydrogen is chemisorption in nature. Sites below the second Pd layer, i.e. interstitial site 3 is a real subsurface site and the interaction between these sites and hydrogen is absorption in nature. The sites much below these subsurfaces are responsible for the hydrogen bulk diffusion. The values of desorption energy for bulk diffusion is ~ 4.4 kcal mol⁻¹ is always

smaller than the energy of desorption from a surface chemisorbed state (20 kcal mol^{-1}) [19]. Hydrogen adsorption on the Pd surface or absorption in its subsurface and/or its alloys occur above 300 K. Hydrogen absorption into the subsurface is responsible for the formation of PdH_x species. The decomposition of PdH_x species during temperature rise occurs at about 373 K. However, the absence of this negative signal in the TPR pattern of Pd/MgO may be due the formation of a over layer of MgO on Pd surface. It is reported that presence of Cl^- ion helps the formation of a MgO over layer on the active components like Cu [10]. TPR pattern of Pd/Cr₂O₃ indicates the presence of $\beta\text{-PdH}_x$ decomposition at around 373 K, and a broad positive signal due to the loss of labile oxygen associated with Cr₂O₃ at high temperatures. TPR studies on Cr₂O₃ indicate the loss of labile oxygen in two stages, one at a T_{max} of 623 K and the other at a T_{max} of 773 K. In the present study, the high temperature reduction maximum ($\sim 973 \text{ K}$) may be due to bulk reduction of Cr₂O₃ to lower oxidation states. It is reported that the reaction of hydrogen with labile oxygen species on the surface of chromia is more likely than the reduction of bulk Cr^{3+} species [20,21]. The amount of labile oxygen species is approximately seven times greater in amorphous chromia than those present on crystalline chromia [21]. In the case of Mg–Cr HT, the reduction process starts at around 773 K probably due to the loss of labile oxygen from Cr₂O₃ phase and the T_{max} is centered nearly at 923 K with unfinished reduction.

Fresh Pd/HT catalysts in their TPR patterns (Fig. 2) exhibit features due to Pd/MgO and Pd/Cr₂O₃. That means, in addition to $\beta\text{-PdH}_x$ decomposition, positive signals due to Cl^- ion reaction in two stages at a T_{max} in the range of 448–548 K and broad signal in the temperature range of 648–773 K are seen. The high temperature signal is attributed to the loss of labile oxygen associated with Cr₂O₃. Among the two unseparable (not well resolved) signals, signal at the low temperature may be due to the reaction of Cl^- ion from the interstitial position of hydrotalcite and the later signal is due the reaction of Cl^- ion from the MgO surface. It is reported that double layered hydroxides with hydrotalcite structure can be synthesized with different contents of Cl^- and CO_3^{2-} anions [22]. However the concentration of Cl^- ion occupying the interstitial positions in between the layers of hydrotalcites may be low and this may be the reason why its presence

is not visible from the XRD patterns of Pd/HT catalysts. The other possibility is the presence of Cl^- ion on Mg–Cr mixed oxide, which is amorphous in nature.

Fig. 3 shows the TPR patterns of Pd/HT used catalysts. It is clearly visible that the intensity of $\beta\text{-PdH}_x$ decomposition signal is higher at higher Pd loadings. Formation of bigger particles of Pd occur at higher loadings, and therefore, high intensity of the signal due to $\beta\text{-PdH}_x$ is not surprising. Evolution of carbonaceous moiety in the form of CH₄ is witnessed when the out let of the TCD is connected in series with a FID detector. The evolution of CH₄ occurs beyond 623 K in three stages. The first two signals with T_{max} occurring in the temperature range of 623–873 K are positive indicating that the carbonaceous moiety is free carbon deposited either on Pd or on support or it can be due to the reduction of PdC_x species. The high temperature signal may be due to the presence of coke like CH_x ($x \geq 2$) species. The nature of carbonaceous moiety is amorphous in nature. However, it is not clear whether it is pyrolytic or acidified carbon or coke.

Fig. 4 shows the effect of Pd loading on Mg–Cr HT in CCl_2F_2 hydrogenolysis activity. From this figure, it is clear that the conversion of CCl_2F_2 increases with Pd loading. The selectivity towards CH_2F_2 and CH_4 increases with Pd loading and remains constant beyond 6 wt.% Pd loading. Thus, 6 wt.% Pd loading is optimum, therefore, chosen for the comparison of its activity with those of Pd/MgO and Pd/Cr₂O₃ catalysts. On this catalyst, the selectivity towards CH_4 is more than that of CH_2F_2 . The selectivities for the two main products, CH_2F_2 and CH_4 have been proposed to be determined by the ratio of the desorption rate of the: CF_2 radical to form CH_2F_2 and the rate of the surface reaction leading to CH_4 . In the reaction scheme proposed by Coq et al. [23] at steady state, the kinetics of CCl_2F_2 hydrogenolysis has been described either by hydrogenation or dehalogenation on the Pd surface by CCl_2F_2 and H_2 , respectively. The promoting effect on Pd for CH_2F_2 formation has been explained in terms of the geometrical effect based on the morphology and size of Pd particles, an electronic influence at the metal/insulator interface and metal–support interaction between Pd and AlF_3 [3,23]. Higher selectivity to CH_2F_2 by the fluoride supported Pd catalysts is attributed to the formation of substoichiometric fluoride moieties at the vicinity or on the Pd particles. The strong acidity of these fluoride

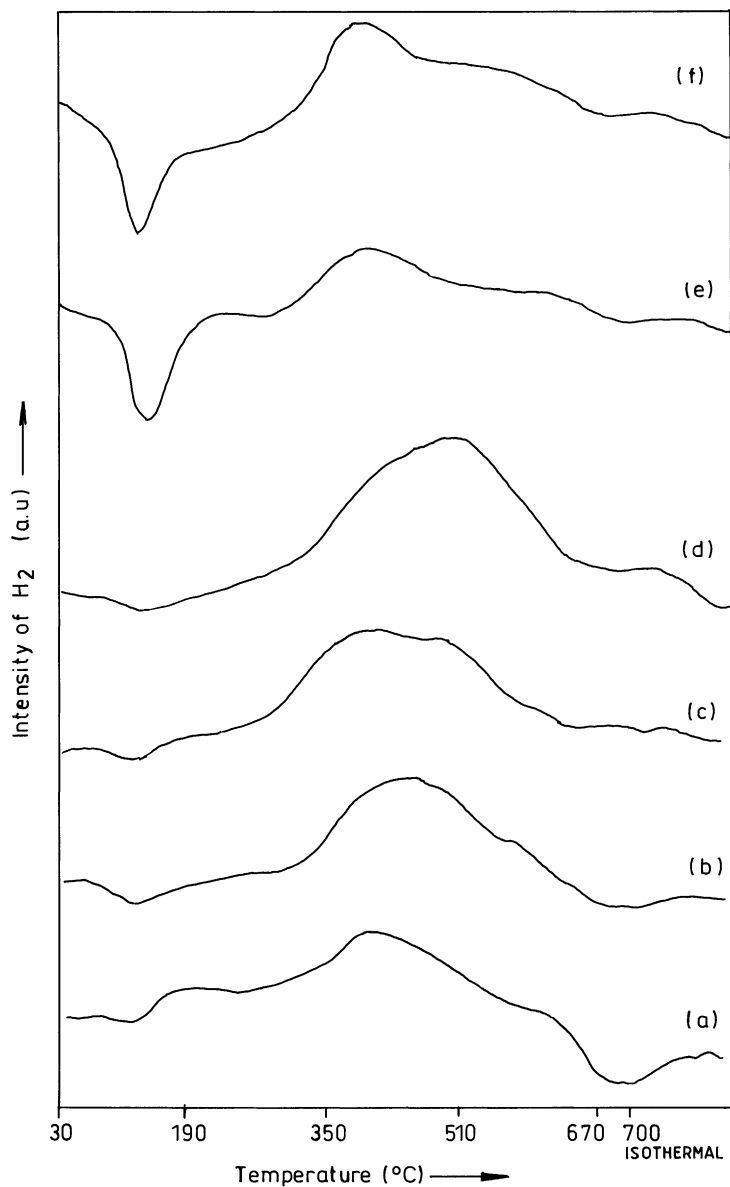


Fig. 3. TPR patterns of used Pd supported on MgO-Cr₂O₃ hydrotalcite catalysts: (a) 1% Pd; (b) 2% Pd; (c) 4% Pd; (d) 6% Pd; (e) 8% Pd; (f) 10% Pd.

species has been reported to favor the desorption of the most abundant surface *CF_2 species upon hydrogen addition, and hence, the selectivity to CH_2F_2 by making the palladium sites more electron deficient. Most probably, the basic character of Pd/HT catalysts favor the rate of the surface reaction leading to CH_4

than the desorption rate of the *CF_2 radical and hence, CH_4 formation is predominant on these catalysts.

Table 2 shows the comparison of activities of Pd/HT, Pd/MgO and Pd/Cr₂O₃ catalysts with 6 wt.% Pd loading. It is observed that the rate of conversion of CCl_2F_2 is more on Pd/HT compared to that over other

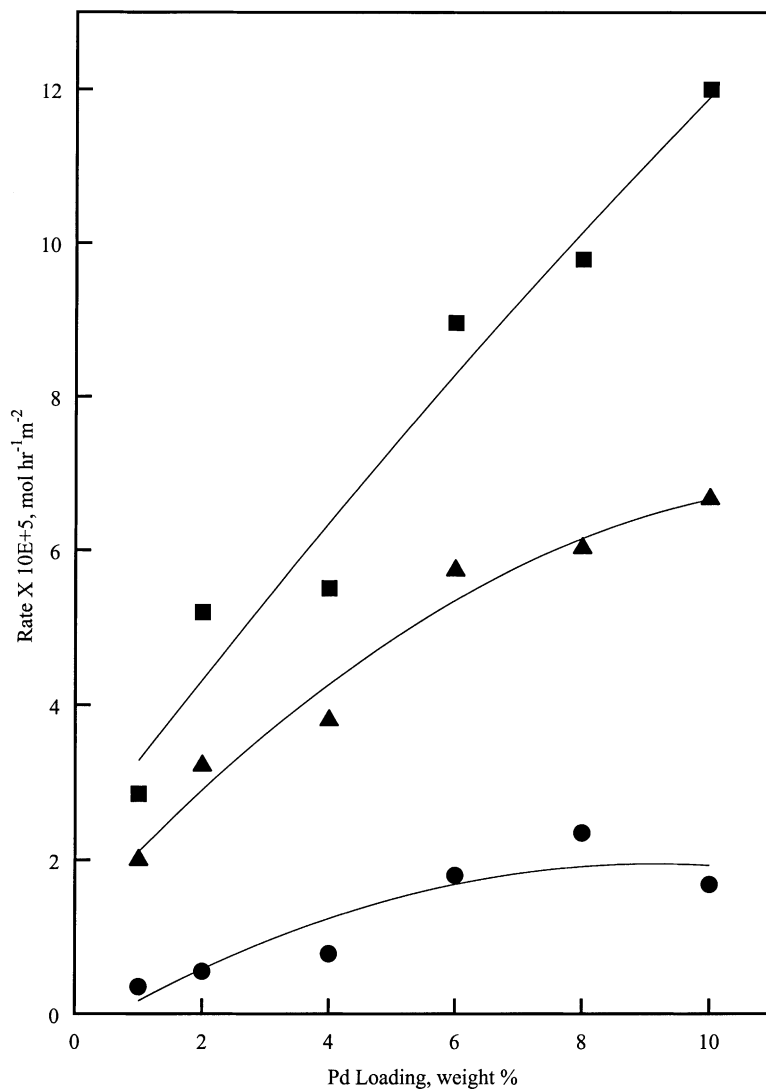


Fig. 4. Effect of Pd loading on the activity of Pd Supported on calcined MgO-Cr₂O₃ hydrotalcite catalysts: (■) rate of R-12 conversion; (▲) rate of CH₄ formation; (●) rate of R-32 formation.

Table 2
Comparison of activities over Pd/MgO, Pd/Cr₂O₃ and Pd/HT catalysts

S. no.	Catalyst	Rate of CCl ₂ F ₂ conversion ($\times 10^5 \text{ mol h}^{-1} \text{ m}^{-2}$)	Rate of CH ₂ F ₂ formation ($\times 10^5 \text{ mol h}^{-1} \text{ m}^{-2}$)	Rate of CH ₄ formation ($\times 10^5 \text{ mol h}^{-1} \text{ m}^{-2}$)
1	Pd/MgO	4.40	2.79	1.28
2	Pd/Cr ₂ O ₃	2.29	1.01	1.16
3	Pd/HT	8.96	1.80	5.74

catalysts. However, this catalyst favors the formation of deep hydrogenated product predominantly. On the other hand, Pd/MgO catalyst favors the formation of dechlorination product. Pd/Cr₂O₃ shows poor catalytic activity in the hydrogenolysis of CCl₂F₂. The synergistic interaction between MgO and Cr₂O₃ in the support obtained upon calcination of hydrotalcite precursor plays an important role in yielding higher rates of CCl₂F₂ conversion selectively to wards the formation of deep hydrogenated products.

4. Conclusions

1. Calcined Mg-Cr hydrotalcite as a support for palladium has shown superior CCl₂F₂ hydrogenolysis activity compared to Pd supported on MgO and Cr₂O₃.
2. Mg-Cr hydrotalcite supported Pd catalyst shows predominantly deep hydrogenation activity resulting in the formation more amount of CH₄ in the hydrogenolysis reaction of CCl₂F₂.
3. Pd supported on MgO has given much higher selectivity to CH₂F₂ (>60%) in the reaction of CCl₂F₂ under H₂.
4. Pd supported on Cr₂O₃ has shown poor activity in the reaction.
5. Calcined Mg-Cr hydrotalcite has shown synergy when used as a support for Pd and used for the hydrogenolysis of CCl₂F₂.
6. From the TPR studies, while β-PdH_x formation is not observed on Pd/MgO catalyst, the same is observed on Pd/Cr₂O₃ and Pd/Mg-Cr hydrotalcite catalyst(s). The absence of β-PdH_x formation on Pd/MgO may perhaps be due to the decoration of MgO layer on Pd particles.

Acknowledgements

UGC and CSIR, New Delhi are gratefully acknowledged by A.H. Padmasri, A. Venugopal and J. Krishna

Murthy for the financial support. The authors thank Dr. K.V. Raghavan, Director, TICT, Hyderabad, for his keen interest in this work.

References

- [1] F. Cavani, F. Trifiro, A. Vaccari, *Catal. Today* 11 (1991) 173.
- [2] R. Shiozaki, T. Hayakawa, Y. Liu, T. Ishii, M. Kumagai, S. Hamakawa, K. Suzuki, T. Itoh, T. Shishido, K. Takehira, *Catal. Lett.* 58 (1999) 131.
- [3] B. Coq, F. Figueras, S. Hub, D. Toumigant, *J. Phys. Chem.* 99 (1995) 11159.
- [4] A. Wiersma, E.J.A.X. van de Sandt, M. Makkee, C.P. luteijn, H. van Bekkum, J.A. Moulijn, *Catal. Today* 27 (1996) 257.
- [5] S.Y. Kim, H.C. Choi, O.B. Yang, K.H. Lee, J.S. Lee, Y.G. Kim, *JCS Chem. Commun.* (1995) 2169.
- [6] A. Malinowski, W. Juszczyk, J. Pielaszek, M. Bonarowska, M. Wojciechowska, Z. Karpinski, *JCS. Chem. Commun.* (1999) 685.
- [7] A.H. Padmasri, A. Venugopal, J. Krishnamurthy, K.S. Rama Rao, P. Kanta Rao, unpublished results.
- [8] S. Velu, C.S. Swamy, *Appl. Catal. A* 162 (1997) 81.
- [9] W.T. Reichle, *J. Catal.* 94 (1985) 547.
- [10] V. Nageswara Rao, P.S. Sai Prasad, K.B.S. Prasad, P. Kanta Rao, *JCS Chem. Commun.* (1990) 278.
- [11] R. Alimann, H.P. Jepson, *Neues Jahrn. Mineral. Monatsh.* (1969) 544.
- [12] S. Miyata, *Clays Clay Miner.* 23 (1975) 369.
- [13] S. Miyata, T. Kumara, H. Hattori, K. tanabe, *Nippon Kayaku Zasshi* 92 (1971) 514.
- [14] P.G. Rouxhet, H.F.W. Taylor, *Chimia* 23 (1969) 480.
- [15] M. Lagos, *Surf. Sci. Lett.* 122 (1982) L601.
- [16] M. Lagos, I.K. Schuller, *Surf. Sci.* 138 (1998) L161.
- [17] M. Lagos, G. Martinez, I.K. Schuller, *Phys. Rev. B* 29 (1985) 5979.
- [18] M.A. Van Hove, K. Hermann, *Surface Architecture and Latuse, A PC Based Programme, Version 2.0, Lawrence Berkeley Lab., Berkeley, LA, USA, 1988.*
- [19] R.J. Behm, V. Penka, M.G. Cattania, K. Christmann, G. Ertl, *J. Chem. Phys.* 78 (1980) 7486.
- [20] H.E. Curry-Hyde, H. Musch, A. Baiker, M. Schraml-Marth, A. Wokaun, *J. Catal.* 133 (1992) 397.
- [21] H.B. Curry-Hyde, H. Musch, A. Baiker, *Appl. Catal.* 65 (1990) 211.
- [22] D. Tichit, M.H. Lhouty, A. Guida, B.H. Chiche, F. Figueras, A. Auroux, D. Bartalini, E. Garrone, *J. Catal.* 152 (1995) 50.
- [23] B. Coq, J.M. Cognion, F. Figueras, D. Toumigant, *J. Catal.* 141 (1993) 21.